Published in final edited form as:
ACS Appl Mater Interfaces. 2012 September 26; 4(9): 4476–4483. doi:10.1021/am301118f.

Asymmetric Free-Standing Film with Multifunctional Anti-Bacterial and Self-Cleaning Properties

Liyan Shen[1,2], **Bailiang Wang**[1], **Jinlei Wang**[1], **Jinhong Fu**[1], **Catherine Picart**[2,*], and **Jian Ji**[1,*]

[1]MOE Key Laboratory of Macromolecular Synthesis and Functionalization, Department of Polymer Science and Engineering, Zhejiang University, Hangzhou 310027, China

[2]LMGP, UMR5628, CNRS and Grenoble Institute of Technology, 3 parvis Louis Néel, F-38016 Grenoble Cedex, France

Abstract

A superhydrophobic/hydrophilic asymmetric free-standing film has been created using layer-by-layer assembly technique. Poly(ethylene-imine)-Ag^+ complex (PEI-Ag^+) at pH 9.0 was assembled with poly(acrylic acid) (PAA) at pH 3.2 on a Teflon substrate to yield a micro-nanostructured surface that can be turned to be superhydrophobic after being coated with a low surface energy compound. Silver nanoparticle loaded free-standing film with one surface being superhydrophobic while the other surface is hydrophilic was then obtained after detachment from the substrate. The superhydrophobicity enabled the upper surface with anti adhesion and self-cleaning properties and the hydrophilic bottom surface can release silver ions as antibiotic agent. The broad-spectrum antimicrobial capability of silver ions released from the bottom surface coupled with superhydrophobic barrier protection of the upper surface may make the free-standing film a new therapy for open wound.

Keywords

Asymmetric; superhydrophobic; free-standing films; anti adhesion; drug release; layer-by-layer assembly

INTRODUCTION

Free-standing films can sustain their shape and other properties in air or liquid after been released from the substrates.[1] Thin free-standing films have aroused great interest because they exhibit dramatically different behavior when compared to bulk materials, with changes in properties such as glass transition,[2-4] transport,[5-7] and stress to failure.[8,9] Meanwhile, free-standing films have found great potential use as sensors,[10,11] barrier materials,[12] reflectors,[13] and electronic films.[14,15] Due to their unique properties including high flexibility, non-covalent adhesiveness, transparency and large aspect ratio, free-standing

*To whom correspondence should be addressed. Prof. Jian JI, Department of Polymer Science and Engineering, Zhejiang University, 310027, Hangzhou, China, Tel/Fax: +86(0)571-87953729, e-mail: jijian@zju.edu.cn; Prof. Catherine PICART, LMGP, CNRS UMR 5628 and Grenoble Institute of Technology, 3 parvis Louis Néel, F-38016 Grenoble Cedex, France, phone: +33(0)4 56 52 93 11, fax: +33(0)4 56 52 93 01, catherine.picart@grenoble-inp.fr.

Europe PMC Funders Author Manuscripts

films have found new use in the biomedical field.[16-23] Fujie et al.[16-18] reported the fabrication of a polysaccharide free-standing film via a spin-coating assisted layer-by-layer method, using alternating deposition of oppositely charged polysaccharides through electrostatic interactions. The polysaccharide free-standing films were proved to be capable to tightly and firmly repair a pleural injury/defect after thoracic surgery so as to prevent air leakage and postsurgical adhesion.[17] Recently, attention has been paid to the asymmetric properties, such as wettability and morphology, for the two surfaces of free-standing films. Lutkenhaus and co-workers[24] fabricated an asymmetric membrane with a fine porous skin layer and a thick microporous underlying layer via acidic postassembly treatment of a linear poly(ethylene-imine)/PAA (LPEI/PAA) multilayer. The same authors[25] also pointed out the possibility of constructing free-standing films with asymmetric wettability just after detachment of Poly(ethylene oxide)/PAA (PEO/PAA) LBL multilayer from substrates. The LBL assembly technique actually provides its attractive advantage to fabricate asymmetric free-standing films since the top and the underlying layer can be easily made of different polyelectrolytes with different structures and functionalities. Multifunctionality is desired for several applications. For example, the cure for wound dressing should be on one hand antibacterial and on the other hand keep the wound from the outer environment. We have previously constructed a humidity responsive free-standing (PEI/PAA) film via pH amplified layer-by-layer assembly.[26] We showed that the film exhibited a fast and reversible humidity responsiveness, which originated from its asymmetric superhydrophobic/hydrophilic wettability. Indeed, we believe that the asymmetric wettability can be explored as more functionality since surface wettability plays a pivotal role in the contact of liquids with solids and in surface adhesion as well. A surperhydrophobic surface is known to be water-repellent and self-cleaning.[27] It provides a barrier to prevent water molecules from penetrating the film and protect it from the outer environment. In addition, the superhydrophobic barrier may also keep water and other moieties from leakage via diffusion, while water and water soluble moieties can be absorbed and/or desorbed by the hydrophilic surface easily.

In this work, a free-standing film loaded with silver nanoparticles with one surperhydrophobic surface and the other being hydrophilic was created via amplified layer-by-layer assembly on hydrophobic polytetrafluoroethylene (PTFE, name here Teflon). The LBL film was subsequently released from the substrate. The anti adhesive and self-cleaning properties of the superhydrophobic upper surface and the bactericidal activity of the hydrophilic surface which extensively release silver ions were studied.

EXPERIMENTAL SECTION

Fabrication of free-standing films

As illustrated in scheme 1, PEI-Ag/PAA multilayer films were built by firstly immersing the Teflon substrate into PEI-Ag^+ solution (1 mg/mL, pH 9.0, Ag^+ 1.6 mM) for 15 min followed by three rinsing with pure water (with pH of approximately 5.5) and dried in a stream of N_2. The substrate was then immersed into PAA solution (3 mg/mL, pH 3.2) for 15 min followed by three washes with pure water and drying. The adsorption and washing steps were repeated until 40 layers were obtained. After that, the multilayer films were placed in a

sealed chamber in the presence of triethoxy-tridecafluoro-n-octylsilane; the sealed chamber was placed in an oven at 130°C for 2.5 hrs. The thermal treatment lead to a thermal crosslinking with the formation of imide bonds.[26] In addition, the reaction with silane and amino groups on film surface via chemical vapor deposition of the silane was realized[26] to obtain surfaces with very low surface energy. Of note, the silver ions incorporated were reduced to silver nanoparticles during the same heating process.[28-30] Finally, the multilayer film was peeled away from the hydrophobic substrate using tweezers. An asymmetric free-standing film with silver nanoparticles was thus obtained (film *a* in scheme 1). For comparison, PET (polyethylene terephthalate) supported films (film *b*, *c* and *d*) were also constructed. As indicated in scheme 1, film *b* was composed of 40 layers and was coated with silane; film *c* was also made of 40 layers but without silane coating as no triethoxy-tridecafluoro-n-octylsilane was present during the thermal treatment process; film *d* was ending with *a* PEI layer (total of 39 layers) and with a silane coating.

Quartz crystal microbalance (QCM)

The PEI-Ag/PAA film buildup process was followed by a quartz crystal microbalance (QTZ, Resonance Probe GmbH, Goslar, Germany). A CHI125A quartz crystal with a fundamental frequency of 8 MHz was obtained from CHI. The electrode was fixed in a special apparatus so that only one side of the electrode was in contact with the solutions (about 0.15 mL). The multilayer films were constructed onto electrodes via the same layer-by-layer deposition as described above. The decrease of the resonance frequency, Δ*F*, was measured for each deposition step in dry state. The Δ*F* was used to determine the adsorbed mass after each immersion step according to the Sauerbrey's equation:[31]

$$-\Delta F = 2F_0^2 \mathrm{A}^{-1}(\mu\rho_0)^{-0.5}\Delta m$$

Where Δ*F* is the measured resonance frequency decrease (Hz), F_0 is the fundamental crystal frequency (8 MHz), A is the geometric area of the QCM electrode (0.196 cm^2), μ is the shear modulus of quartz (2.947×10^{11} g cm^{-1} s^{-2}), ρ_0 is the density of the crystal (2.648 g cm^{-3}), and Δ*m* is the mass change (g).

Scanning Electron Microscopy (SEM)

The surface morphology of PET supported films and the top and bottom surfaces as well as the cross-section of the $(PEI\text{-}Ag/PAA)_{20}$ free-standing film was imaged using a field emission scanning electron microscope (FESEM; FEI, SiRion100). To follow film growth, (PEI-Ag/PAA) film was also built on silicon substrate. The film thicknesses at after a given number of deposited layer pairs ((4, 5, 6, 7 and 8) were measured by SEM on the film cross-section. All the samples were sputered with a layer of gold before imaging.

Transmission Electron Microscopy (TEM)

The state of silver nanoparticles in the film was confirmed by transmission electron microscopy. For TEM imaging, the free-standing multilayer filsm incorporating silver nanoparticles was immersed in hydrofluoric acid (HF) solution and was immediately withdrawn. The droplet was collected on copper TEM grids, which were subsequently dried

by blotting. The copper TEM grids were then coated with a thin layer of carbon in a thermal evaporator. TEM images were obtained with a JEOL JEM-2000FX operated at 180 kV. From the TEM images, particle size was measured and size distribution was deduced using Image J software v1.38x (NIH Bethesda, USA, http://rsbweb.nih.gov/ij/index.html). More than 150 particles were counted.

Water Contact Angle

Surface wettability for both free-standing and supported films was determined via sessile drop contact angle (CA) measurements taken with a KRUSS DSA 100-MK2 contact angle system at ambient temperature. At five different positions, a 4 μL water droplet was dispensed onto the substrate and the CA was measured and averaged for each sample.

Inductively Coupled Plasma Mass Spectrometry (ICP-MS)

Silver ions release was carried out by immersing pieces of 5×5 mm^2 free-standing $(PEI\text{-}Ag/PAA)_{20}$ films in to 50 mL PBS at 37°C. For PET supported films, $(PEI\text{-}Ag/PAA)_{19}$-PEI-Ag or $(PEI\text{-}Ag/PAA)_{20}$ films with or without silane coating were studied in the same conditions. The Ag^+ concentrations at different release times were measured using ICP-MS PQ3 (X II, Thermo Scientific). To measure the total Ag NPs loading amount, a 5×5 mm^2 piece of film was dissolved in 1 mL HNO_3 and diluted to 50 mL, then the silver ion concentrations were determined by ICP-MS.

Bacteria Initial adhesion

The bacterial strain used herein was *Escherichia coli* (*E. Coli* BL21). The PET supported films were immersed in a bacterial suspension (10 ml) of 10^6 cells per mL in a sterile test tube. The test tube was then shaken at 37 °C for 4 h. After that the samples were taken out and washed three times with sterile PBS. The bacteria were then fixed in 3% glutaraldehyde for 30 min followed by step dehydration using 25%, 50%, 70%, 95% v/v water/ethanol mixture and finally pure ethanol. The samples were imaged by a field emission scanning electron microscopy (FESEM; FEI, SiRion100) after sputtering a thin gold layer. The number of *E. Coli* adhered on the samples were counted from the SEM images taken at magnification of 5000. At lease 6 images were counted to give an average number for each sample.

Bactericidal Activity of the films

The bactericidal activity of the silver NPs incorporated films was tested using a Kirby-Bauer assay.[32] Briefly, the solid slabs of agar made from Cation-adjusted Mueller Hinton Broth II (CMHB) media and BactoAgar were used for bacterial culturing. 1000 cells were planted on each plate, on which free-standing film bottom surface as well as PET supported films were placed film upside down. The plates were incubated at 37 °C overnight and then the inhibition zones were measured. All experiments were done in triplicate.

Self-cleaning property of the films

To test the self-cleaning property of the superhydrophobic film, dusts were put on the film (around 4×4 cm^2) and water was added dropwise until all the dusts were removed. For comparison, Teflon sheet with the same dimension was used as control.

Digital camera images and videos were captured by Sony digital camera (SONY-H 9).

RESULTS AND DISCUSSION

Fabrication of silver NPs loaded free-standing film

We have previously reported the construction of superhydrophobic multilayered films via silver ion amplified exponential growing layer-by-layer deposition.[33,34] Here we employed the same protocol while slightly increased the pH of PAA deposition solution, so that part of silver ions can still be captured in the films (see Table SI1). As shown in scheme 1, poly(ethylene imine)-Ag^+ complex (PEI-Ag^+) at pH 9.0 and poly(acrylic acid) (PAA) under pH 3.2 were alternately deposited onto Teflon substrate to form mutlayers (with 40 layers). The films were then cross-linked by heating and coated with triethoxy-tridecafluoro-n-octylsilane to reduce surface energy via chemical vapour deposition. Meanwhile, the silver ions incorporated were reduced to be silver nanoparticles,[28,29] which can serve as the source for Ag^+ release.[35] Finally, the free-standing films (film *a*) with inverse wettability were obtained by peeling them away from the Teflon substrates with tweezers. When the PET substrate was used, supported films with either rough (film *b* and *c*) or flat (film *d*) surface morphology depending on the outermost layer were constructed.

In order to sustain themselves as free-standing, the films should be mechanically strong enough or thick enough. In our system, Ag^+ amplified LBL exponential growth guarantees the fast fabrication of thick multilayer in a limited deposition cycles. The QCM data and cross-section measurements from SEM revealed that the film mass and thickness increased exponentially with the increase of deposition layers due to the diffusion “in” and “out” of PEI chains. The addition of Ag^+ can further enlarged the diffusion ability of PEI and amplified the exponential growth.[33] As shown in Figure 1, the thickness of an 8-bilayer film was 8.25 μm on hydrophilic silicon wafer. The films on Teflon substrate grew much more slowly because of poor adsorption of hydrophobic substrate for the initial layers. Nevertheless, the thickness of a (PEI-Ag/PAA) film made of 20 layer pairs was of 19.5 ± 1.6 μm after peeling off from the Teflon substrate, as indicated in Figure 2 A. The free-standing film can be transferred to most liquid/air or solid/air interface including the human tissues easily, especially in wet state. As shown in Figure 2 B, the free-standing film was flexible and attached easily to human skin through its bottom surface, which was previously in contact with the Teflon substrate. SEM was also applied to monitor the surface morphology for different films (Figure 3). The enhanced “in” and “out” diffusion of PEI via addition of silver ions coupled with pH change not only resulted in the amplification of exponential growth but also in a change of the morphology of the multilayer. Indeed, surface morphology changed from very rough to relatively flat (see Figure SI1). When the film ended with PAA, the PEI molecules in the film diffused out to complex the incoming PAA chains, which cannot diffuse, in film/liquid interface. This resulted in a hierarchically rough

surface. Figure 3 A shows that the surface, which was far away from substrate (indicated as top surface), exhibited a micro nano-hierarchical topography while the other surface previously attached to the substrate (indicated as the bottom surface) was relatively smooth with some microscale structures (Figure 3 B). Obviously, the top surface was homogeneously covered with 2-5 μm wormlike features, in which many granular nanostructures and nano-pores were observed. These micro- and nano-structures were crucial for creating superhydrophobic surfaces. The surface morphology of film *b* was similar to the top surface of film *a*, as can be seen in Figure 3 C. A silane coating did not change the film surface morphology. The morphology of film *c* was identical to that of film *b* (data not shown). For film *d*, which is ending with PEI-Ag, the surface was flat (Figure 3 D) as the diffusion of PEI chains during PEI-Ag^+ deposit steps filled up the empty spaces in PAA-ending film and released the isolated PEI-PAA complex structures.

In Figure 3 D, we also noticed that silver particles covered the film surface after thermal treatment. The formation of silver nanoparticles in free-standing films was further confirmed by TEM observations. The silver NPs containing droplets were collected on TEM copper grids after dissolving partial of the free-standing film in HF solution. As shown in Figure 4, the size of the silver particles ranged from 5 nm to about 50 nm with an average diameter of 23 nm.

Asymmetric wettability of the free-standing film

Water contact angles for free-standing films as well as PET-supported films were measured and listed in table 1. After coated with triethoxy-tridecafluoro-n-octylsilane, the surface energy was greatly reduced. In addition, the water contact angle on the hierarchically structured surface of the free-standing film was as high as 168.2°, indicating it was superhydrophobic whereas that of the bottom surface was relatively low at 52.7°. The sharp difference in wettability lead to very different behaviors of the two surfaces when set in contact with water. Two pieces of free-standing films were put in water, one with its top surface facing air (the left one in Supporting information 2) and the other with the bottom surface facing air (the right piece in Supporting information 2). Both films were well spread at the air-water interface. When water droplets were deposited onto the films, the water droplet on the top (superhydrophobic) surface remained a sphere for a long time, as anticipated, whereas a water droplet on the bottom surface was gradually absorbed into the film. After ~ 16 s, the 15 μL droplet disappeared on the bottom surface.

Water contact angle for film *b*, *c* and *d* were 169.2°, 126.2° and 112.1°, respectively. Considering the similarity of both surface morphology and wettability, film *b* can represent the properties of the top surface of the free-standing film. Film *c* had a rough surface morphology but was hydrophobic. By comparing the superhydrophobic film (film *b*) and rough hydrophobic film (film *c*), we could get some information about the effect of silane coating. Meanwhile, the role of surface structure can be appreciated by comparing the superhydrophobic film (film *b*) to the flat hydrophobic film (film *d*). Of note, the PEI-Ag ending film was also hydrophobic even without silane coating (CA = 98.6°). This may be due to a reorganization of the hydrophobic groups in the film toward the film surface, during thermal treatment.[34]

Bactericidal Activity of the bottom surface

The amount of Silver NPs loaded in the free-standing $(PEI\text{-}Ag/PAA)_{20}$ film was 2.17 ± 0.08 g/cm^2 determined by ICP-MS. When the film was immersed in solution, the silver nanoparticles incorporated were eroded and released as Ag^+.[35] The silver ions release behavior of both supported and free-standing films was tested. As demonstrated in figure 5 A, the free-standing film (film *a*) released silver ions rapidly and most of its silver ions were released in the first 12 hrs. In contrary, for PET supported superhydrophobic $(PEI\text{-}Ag/PAA)_{20}$ film (film *b*), only 6% of the total silver was released in 48 hrs. These differences between film *a* and film *b* clearly demonstrated that most of the Ag^+ in free-standing film was released from the bottom (hydrophilic) surface. To further understand the Ag^+ entrapment, the silver ions release behavior was also investigated for PET-supported hydrophobic films with rough (film *c*, PAA-ending without silane coating) or flat (film *d*, PEI-ending with silane coating) surfaces. As shown in figure 5 A, silver ions released quickly from film *c* (PAA-ending without silane coating). Indeed, this film released 89% of its Ag^+ content in 48 hrs. Compared to the lowest release for film *b* (PAA-ending with silane coating), which released only 6% of its silver, it is clearly demonstrated that the silane coating was important for Ag^+ entrapment. However, the micro-nano structure of the surfaces also contributed to the entrapment of Ag^+. Film *d*, which is PEI-Ag^+ ending and coated with silane, can still release silver ions but in a much more gradual fashion (~ 59% release in 48 hrs). Wetting plays a very important role in the release of water soluble moieties embedded within the film, such as Ag^+ here. For the bottom (hydrophilic) surface of free-standing film, water can diffuse in the film and this facilitated the ion release process. In contrary, for the top (superhydrophobic) surface, as water could not wet it, the release of Ag^+ was greatly inhibited.

Of note, neither the micro-nano structure on film surface alone (e.g. PAA-ending film without silane, CA=126.2°) nor a low surface energy coating alone (e.g. PEI-Ag-ending film with silane, CA=112.1°) can effectively prevent the release of Ag^+ ions. But combining micro-nano structure with silane coating could effectively prevent silver ions from releasing. Therefore, the asymmetric film with inverse superhydrophobic/hydrophilic wettability delivered Ag^+ one-directionally from the bottom surface.

Silver ion is known as a wide-spectrum anti-bacterial agent.[36] The bactericidal activity of the silver NPs loaded films was examined by a Kirby-Bauer assay[32] using *E. Coli*. As indicated in Figure 5, inhibition zones were found for samples with Ag NPs but no inhibition zone was observed for film without Ag NPs (Figure 5 B'). While a big inhibition zone of 8.9 mm was found when the bottom surface of film *a* was turned up (figure 5 B), the inhibition zone decreased drastically to 1.8 mm for film *b* which is supposed to be similar as the top surface of film *a* (Figure 5 C). It is not difficult to understand the results if we consider the relationship between the inhibition zone and the amount of relative released silver ion of different samples (Figure 5 F). And the results of the Kirby-Bauer assay confirmed again the asymmetric release rate of Ag^+ from the asymmetric free-standing film, which will lead to asymmetric anti-bacterial ability.

Self-cleaning ability of the upper surface

Superhydrophobic surfaces are also well known as self-cleaning[27] like lotus leaves, which can get rid of dusts in the presence of water droplets. The self-cleaning property of PET supported suprhydrophobic $(PEI\text{-}Ag/PAA)_{20}$ film (film *b*) was examined. The hydrophobic Teflon substrate, which is a commercially available self-cleaning material, was chosen here as control. The substrates were initially covered with dusts (Figure 6 A and B). When water was added dropwise on the film, the droplet rolled down from the film surface and took away the dusts on its path. After adding 3 mL water, all the dusts on the film surface had been taken away (Figure 6 A'). In comparison, for the Teflon substrate, water droplet slid down on the surface and could not remove the dusts. Even after addition of 7 mL water, the dusts were still on Teflon surface (Figure 6 B'). (Video was shown in supporting information 3)

Furthermore, the superhydrophobic surface exhibited anti-adhesive properties for microorganism. Thus, the initial *E. Coli* adhesion on PET supported and silane coated films with either PAA-ending or PEI-ending was tested. As illustrated in Figure 7, *E. Coli* adhered separately on PET substrate but aggregated on $(PEI/PAA)_{19}$-PEI surface (Figure 7 B). When *E.Coli* was incubated with $(PEI\text{-}Ag/PAA)_{19}$-PEI-Ag film (Figure 7 C), less bacteria were found on the surface compared to $(PEI/PAA)_{19}$-PEI film, and the bacteria were not in a normal shape. This may because the bacteria were killed by the released silver ions. Interestingly, almost no *E. Coli* was be found on the PAA-ending films with silane coating containing or no silver (Figure 7 D, E). The excellent anti-adhesion ability may come from the combination of micro-nano structure and superhydrophobicity. Indeed, Cao et al. have revealed that the settlement of zoospores of *Ulva* was strongly influenced by the size of the features present on the surfaces.[37] The lowest level of settlement was observed for structures of the order of 2 μm, a size similar to that of the spores of *Ulva*. Furthermore, the lowest settlement strength was on the surface with the sub-micrometer-sized features. This may be explained by the inability of the adhesive to thoroughly bond to the entire surface area provided. Here, we prove that the combination of micro-nano hierarchical structure and superhydrophobicity can lead to anti bacteria adhesion. Of note, the size of micro-structure on the PAA-ending film here was ~2-5μm, close to the size of *E. Coli*.

CONCLUSIONS

In conclusion, we have demonstrated a facile method for creating asymmetrical free-standing films via amplified layer-by-layer assembly. The free-standing films have asymmetric surface morphology, which resulted in asymmetric wettability: the top surface being superhydrophobic while the bottom one being hydrophilic. The superhydrophobic surface was proved to limit bacterial adhesion and to be self-cleaning, while the hydrophilic surface could extensively deliver bactericidal silver ions. Importantly, the film can be transferred to another interface, such as human skin. Therefore, these asymmetric, multifunctional films may be of great potential for use as patches for open wound, as well as in the area of barrier, separation, transportation or drug delivery.

Supplementary Material

Refer to Web version on PubMed Central for supplementary material.

Acknowledgments

CP thanks the “Institut Universitaire de France” and the European Commission (FP7) via a European Research Council starting grant (BIOMIM, GA 259370) for financial support. LS thanks the French government for financial support through a “Eiffel Doctorat” fellowship, the Rhône-Alpes region through a CMIRA fellowship, and the French Embassy in China. JJ thanks the financial support from the NSFC-50830106, the National Basic Research Program of China (2011CB606203) and China National Funds for Distinguished Young Scientists (51025312).

REFERENCES AND NOTES

(1). Jiang CY, Tsukruk VV. Adv. Mater. 2006; 18:829–840.
(2). Bohme TR, de Pablo JJ. J. Chem. Phys. 2002; 116:9939–9951.
(3). Torres JA, Nealey PF, de Pablo JJ. Phys. Rev. Lett. 2000; 85:3221–3324. [PubMed: 11019306]
(4). Guerin G, PruD’Homme RE. J.Polym. Sci., Part B-Polym. Phys. 2007; 45:10–17.
(5). Huang JJ, Keskkula H, Paul DR. Polymer. 2004; 45:4203–4215.
(6). Huang Y, Paul DR. J. Membr. Sci. 2004; 244:167–178.
(7). Lutkenhaus JL, McEnnis K, Hammond PT. Macromolecules. 2007; 40:8367–8373.
(8). Jiang CY, Markutsya S, Tsukruk VV. Adv. Mater. 2004; 16:157–161.
(9). Markutsya S, Jiang CY, Pikus Y, Tsukruk VV. Adv. Funct. Mater. 2005; 15:771–780.
(10). Jiang CY, Markutsya S, Pikus Y, Tsukruk VV. Nat. Mater. 2004; 3:721–728. [PubMed: 15448680]
(11). Mitsuishi M, Ishifuji M, Endo H, Tanaka H, Miyashita T. Mol. Cryst. Liq. Cryst. 2007; 471:11–19.
(12). Letendre M, D’Aprano G, Lacroix M, Salmieri S, St-Gelais D. J. Agric. Food Chem. 2002; 50:6017–6022. [PubMed: 12358474]
(13). DeCorby RG, Ponnampalam N, Nguyen HT, Clement TJ. Adv. Mater. 2007; 19:193–196.
(14). Shim BS, Tang ZY, Morabito MP, Agarwal A, Hong HP, Kotov NA. Chem. Mater. 2007; 19:5467–5474.
(15). Park J, Kim J, Lee S, Bang J, Kim BJ, Kim YS, Cho J. J. Mater. Chem. 2009; 19:4488–4490.
(16). Fujie T, Okamura Y, Takeoka S. Adv. Mater. 2007; 19:3549–3553.
(17). Fujie T, Matsutari N, Kinoshita M, Okamura Y, Saito A, Takeoka S. Adv. Funct. Mater. 2009; 19:2560–2568.
(18). Fujie T, Kinoshita M, Shono S, Saito A, Okamura Y, Saitoh D, Takeoka S. Surgery. 2010; 148:48–58. [PubMed: 20117815]
(19). Okamura Y, Kabata K, Kinoshita M, Saitoh D, Takeoka S. Adv. Mater. 2009; 21:4388–4392.
(20). Okamura Y, Fukui Y, Kabata K, Suzuki H, Handa M, Ikeda Y, Takeoka S. Bioconjugate Chem. 2009; 20:1958–1965.
(21). Okamura Y, Utsunomiya S, Suzuki H, Niwa D, Osaka T, Takeoka S. Colloids Surf. A: Physicochem. Eng. Aspects. 2008; 318:184–190.
(22). Mattoli V, Pensabene V, Fujie T, Taccola S, Menciassi A, Takeoka S, Dario P. Procedia Chem. 2009; 1:28–31.
(23). Podsiadlo P, Qin M, Cuddihy M, Zhu J, Critchley K, Kheng E, Kaushik AK, Qi Y, Kim H-S, Noh S-T, Arruda EM, Waas AM, Kotov NA. Langmuir. 2009; 25:14093–14099. [PubMed: 19824626]
(24). Lutkenhaus JL, McEnnis K, Hammond PT. Macromolecules. 2008; 41:6047–6054.
(25). Lutkenhaus JL, Hrabak KD, McEnnis K, Hammond PT. J. Am. Chem. Soc. 2005; 127:17228–17234. [PubMed: 16332070]
(26). Shen L, Fu J, Fu K, Picart C, Ji J. Langmuir. 2010; 26:16634–16637. [PubMed: 20879748]

(27). Feng L, Li S, Li Y, Li H, Zhang L, Zhai J, Song Y, Liu B, Jiang L, Zhu D. Adv. Mater. 2002; 14:1857–1860.

(28). Dai J, Bruening ML. Nano Lett. 2002; 2:497–501.

(29). Taylor PL, Omotoso O, Wiskel JB, Mitlin D, Burrell RE. Biomaterials. 2005; 26:7230–7240. [PubMed: 16005958]

(30). Wang TC, Rubner MF, Cohen RE. Langmuir. 2002; 18:3370–3375.

(31). Sauerbrey G. Z. Phys. 1959; 155:206–222.

(32). Bauer AW, Kirby WM, Sherris JC, Turck M. Am. J. Clin. Pathol. 1966; 45:493–496. [PubMed: 5325707]

(33). Ji J, Fu JH, Shen JC. Adv. Mater. 2006; 18:1441–1444.

(34). Fu J, Ji J, Shen L, Küller A, Rosenhahn A, Shen J, Grunze M. Langmuir. 2009; 25:672–675. [PubMed: 19177642]

(35). Liu J, Hurt RH. Environ. Sci. Technol. 2010; 44:2169–2175. [PubMed: 20175529]

(36). Feng QL, Wu J, Chen GQ, Cui FZ, Kim TN, Kim JO. J. Biomed. Mater. Res. 2000; 52:662–668. [PubMed: 11033548]

(37). Cao X, Pettitt ME, Wode F, Sancet MPA, Fu J, Ji J, Callow ME, Callow JA, Rosenhahn A, Grunze M. Adv. Funct. Mater. 2010; 20:1984–1993.

Europe PMC Funders Author Manuscripts

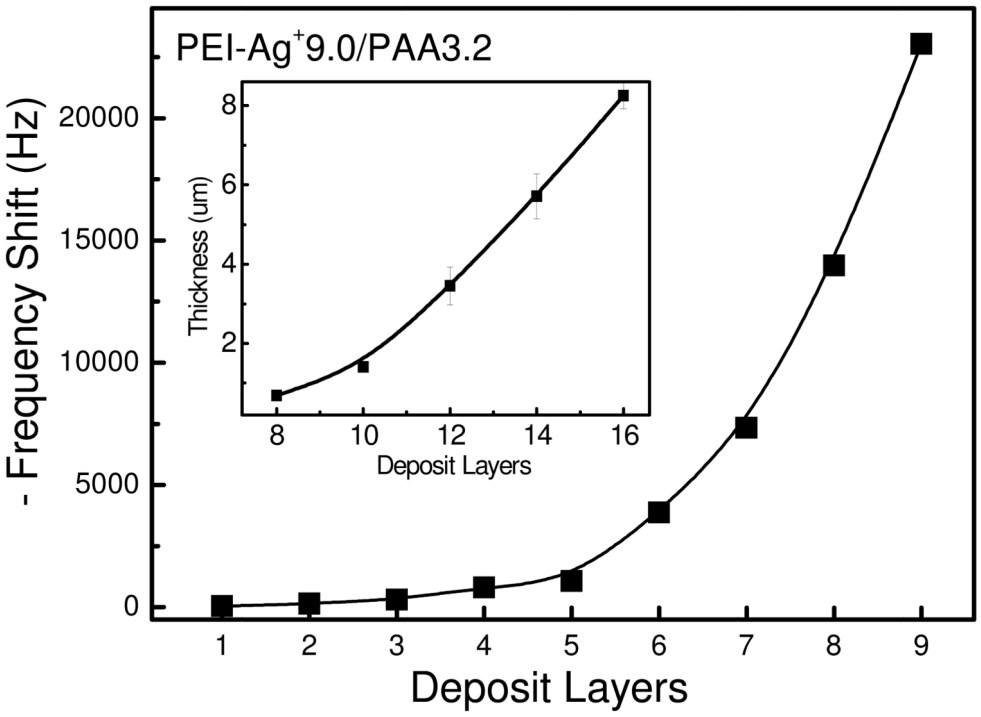

Figure 1.

Growth of a PEI-Ag^+/PAA (pH 9.0/3.2) film followed by QCM. Insert: Thickness of a PEI-Ag^+/PAA (pH 9.0/3.2) film deposited on silicon and measured by SEM.

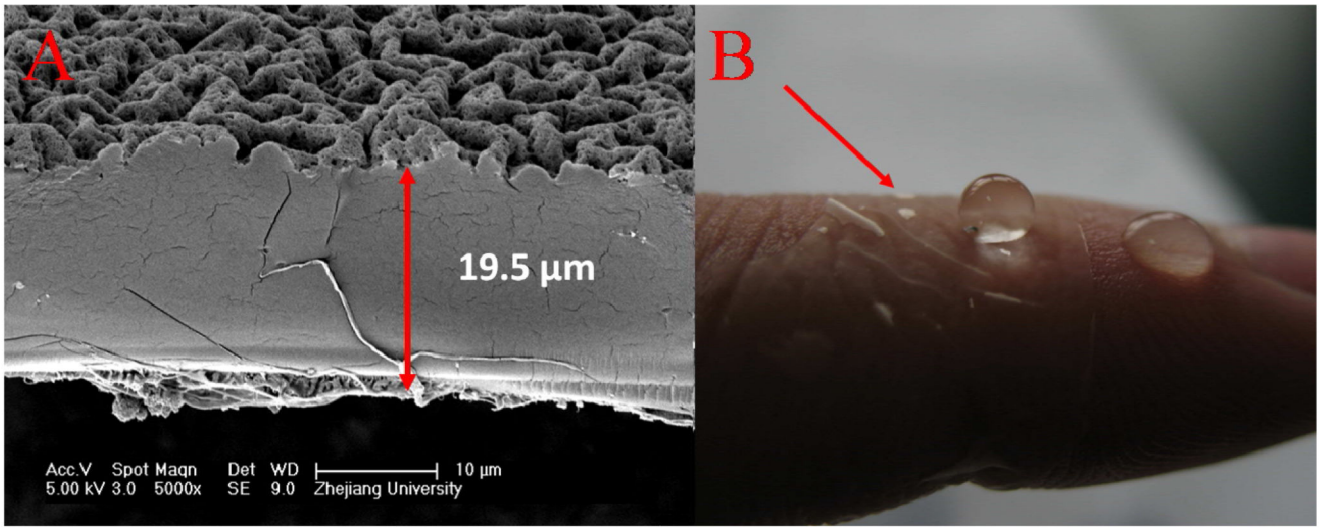

Figure 2.

(A) SEM image of the cross-section of free-standing $(PEI\text{-}Ag/PAA)_{20}$ film. (B) Digital photo of a free-standing $(PEI\text{-}Ag/PAA)_{20}$ film deposited on skin of finger. The top surface is superhydrophobic and the film is transparent.

Europe PMC Funders Author Manuscripts

Europe PMC Funders Author Manuscripts

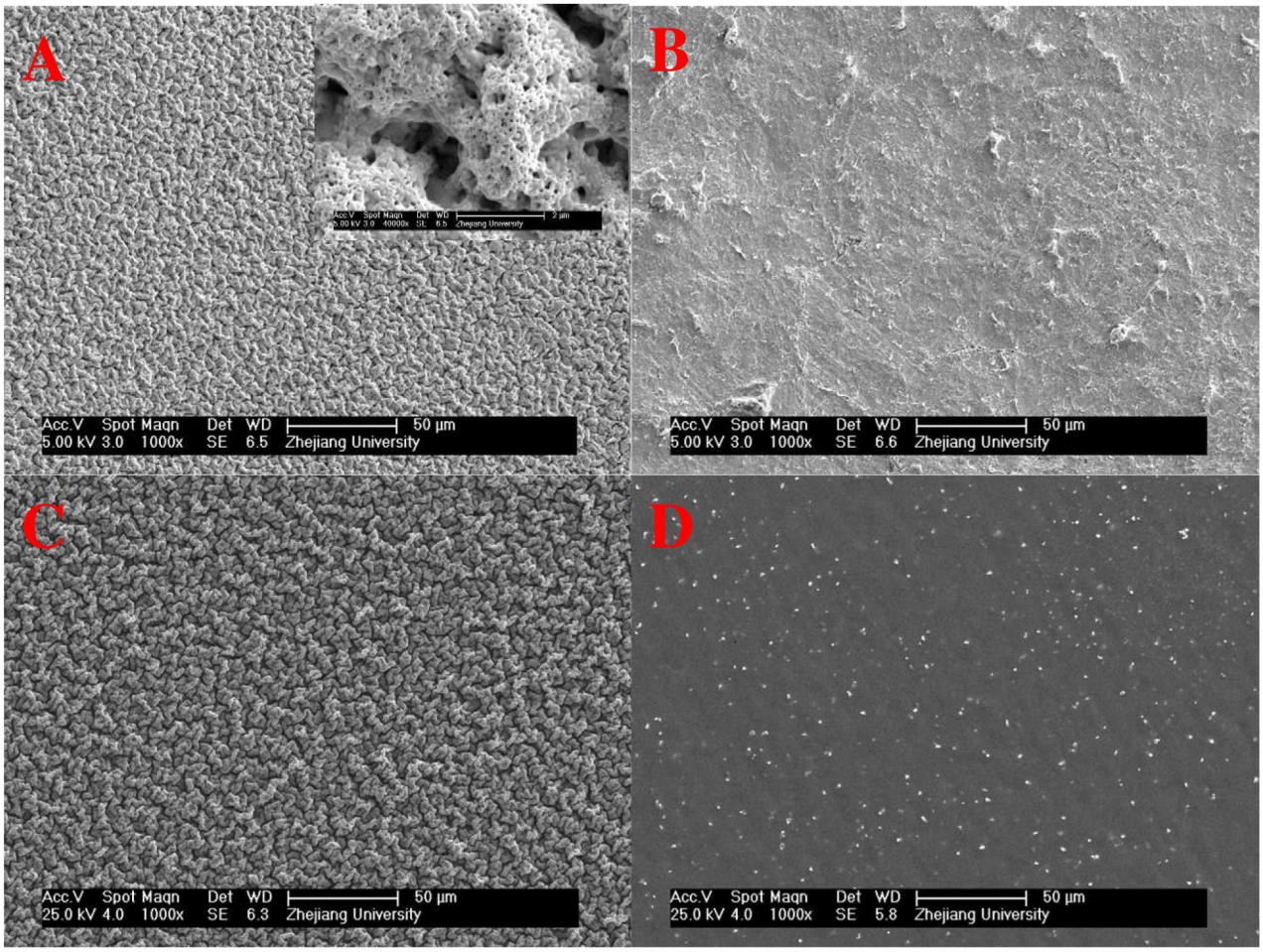

Figure 3.

SEM images of film surface morphology for the top surface (A) and bottom surface (B) of free-standing $(PEI\text{-}Ag/PAA)_{20}$ film (film a) as well as PET supported $(PEI\text{-}Ag/PAA)_{20}$ film (film b) (C) and $(PEI\text{-}Ag/PAA)_{19}$-PEI-Ag film (film d) (D).

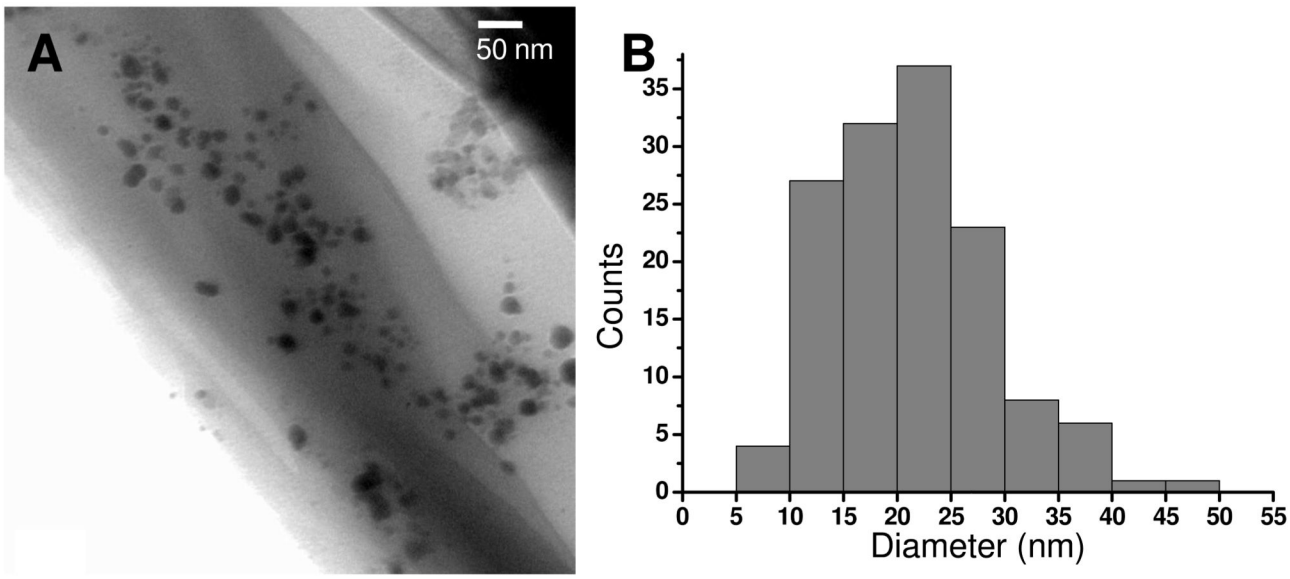

Figure 4.

A, TEM image of silver nanoparticles in the free-standing $(PEI\text{-}Ag/PAA)_{20}$ film after dissolution of the film in HF. B, size distribution deduced from TEM images.

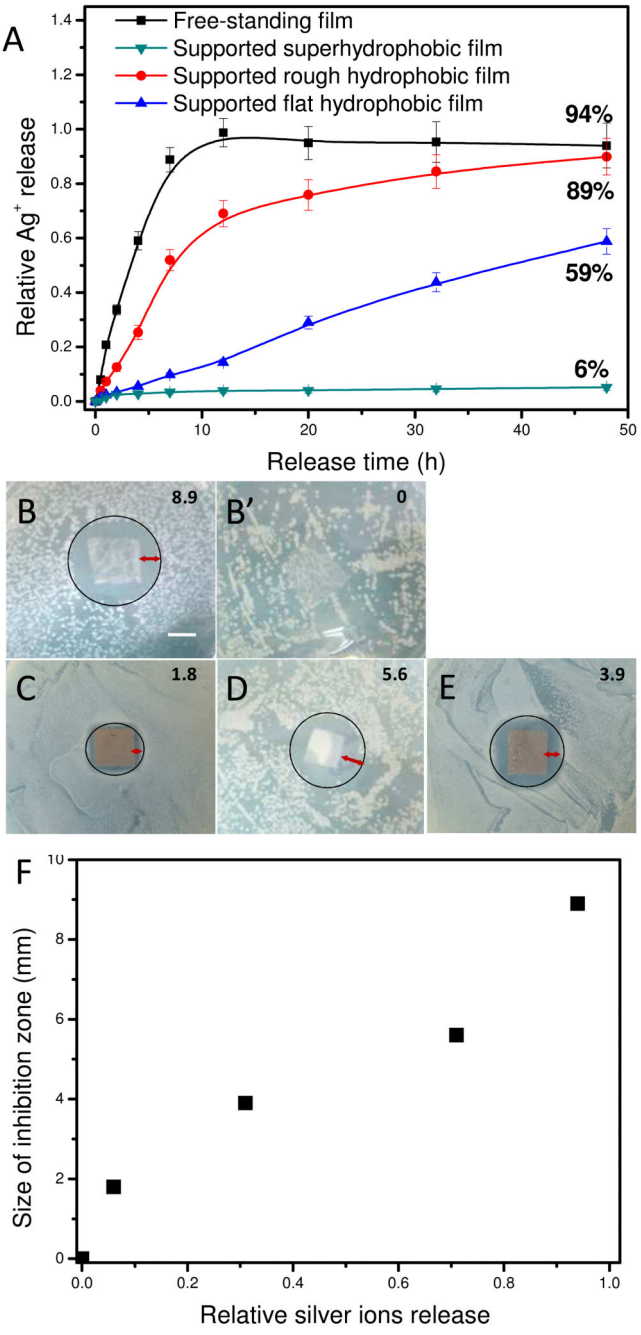

Figure 5.

(A) Silver ion release in percentage for different films including free-standing (PEI-Ag/PAA)$_{20}$ film (■), (PEI-Ag/PAA)$_{20}$ film adhering to PET without silane (●) and with silane (▼), PET supported (PEI-Ag/PAA)$_{19}$-PEI-Ag film with silane (▲). (B, B', C, Dand E) *E. Coli* inhibition zone on agar nutrition with the bottom (hydrophilic) surface of a free-standing (PEI-Ag/PAA)$_{20}$ film (film a) (B) and a free-standing (PEI/PAA)$_{20}$ film (B'), PET supported (PEI-Ag/PAA)$_{20}$ film (film b) (C) and (PEI-Ag/PAA)$_{19}$-PEI-Ag film (film d) (E) with silane, PET supported (PEI-Ag/PAA)$_{19}$-PEI-Ag film (film c) (D) without silane. The

sizes of inhibition zone were 8.9, 0, 1.8, 5.6 and 3.9 mm for B, B', C, D and E, as indicated in the right top corner of the images, respectively. (F) Plot of the inhibition zone sizes against relative silver ions release. Scale bar in B is 1 cm.

Europe PMC Funders Author Manuscripts

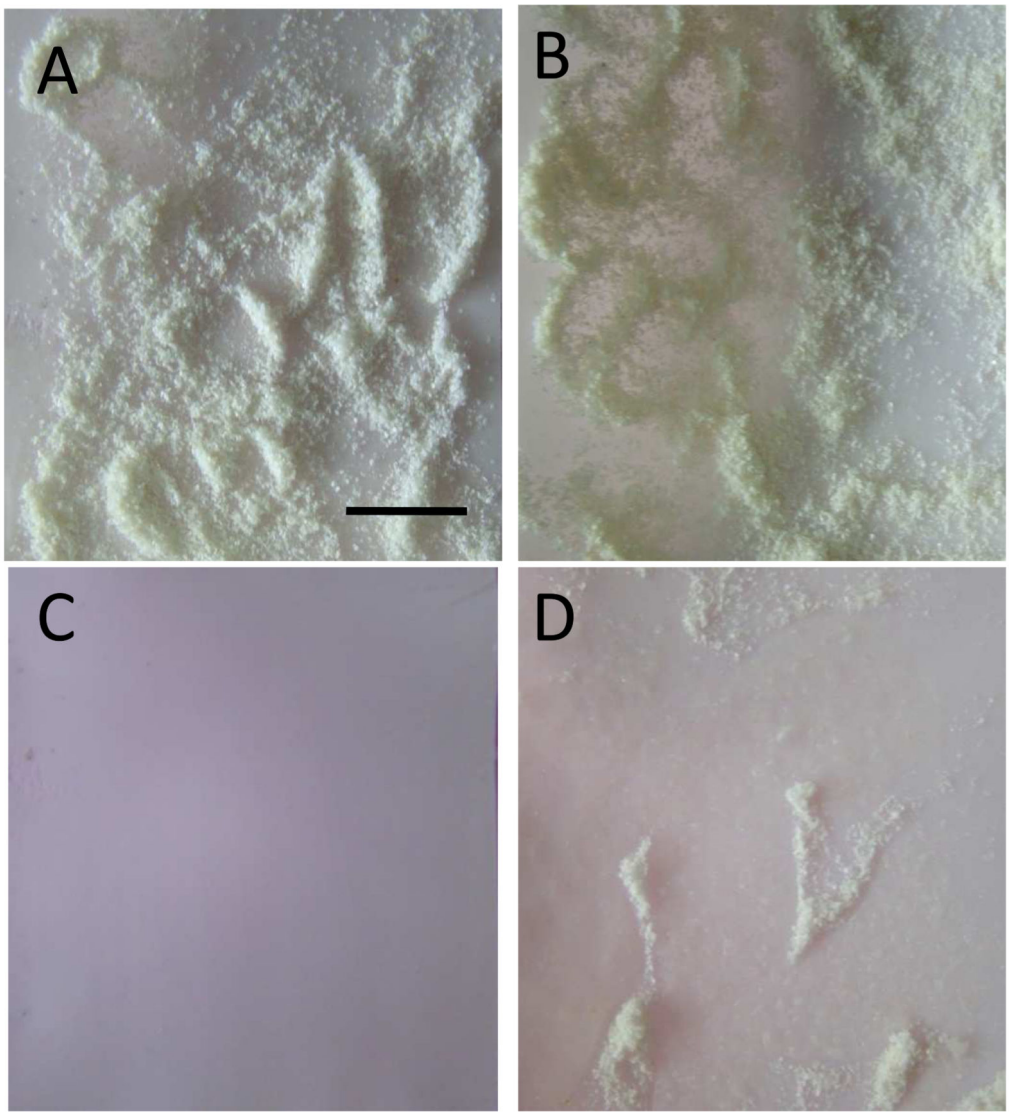

Figure 6.

Digital images of superhydrophobic $(PEI\text{-}Ag/PAA)_{20}$ film on PET (A, A') and PTFE (B, B') with dust (A, B) and after adding 3 mL (A') and 7 mL (B') of water dropwise. Scale bar in A is 1 cm.

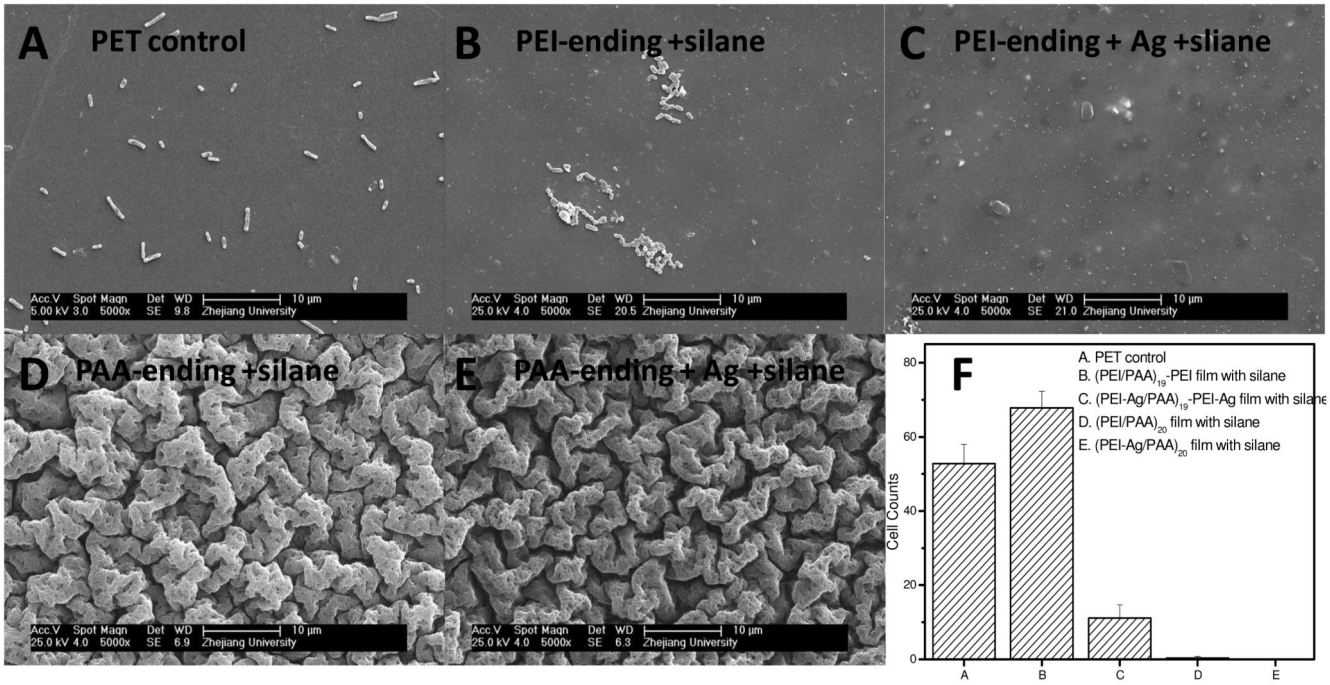

Figure 7.

SEM images of PET supported (PEI/PAA) films after incubation in *E.Coli* solution for 4 h. (A) PET control; (B) $(PEI/PAA)_{19}$-PEI film with silane deposition; (C) $(PEI\text{-}Ag/PAA)_{19}$-PEI-Ag film with silane deposition, (D) $(PEI/PAA)_{20}$ film with silane deposition, (E) $(PEI\text{-}Ag/PAA)_{20}$ film with silane deposition. (F) Corresponding bacterial counts on the different samples, averaged from 6 images for each sample.

Europe PMC Funders Author Manuscripts

Europe PMC Funders Author Manuscripts

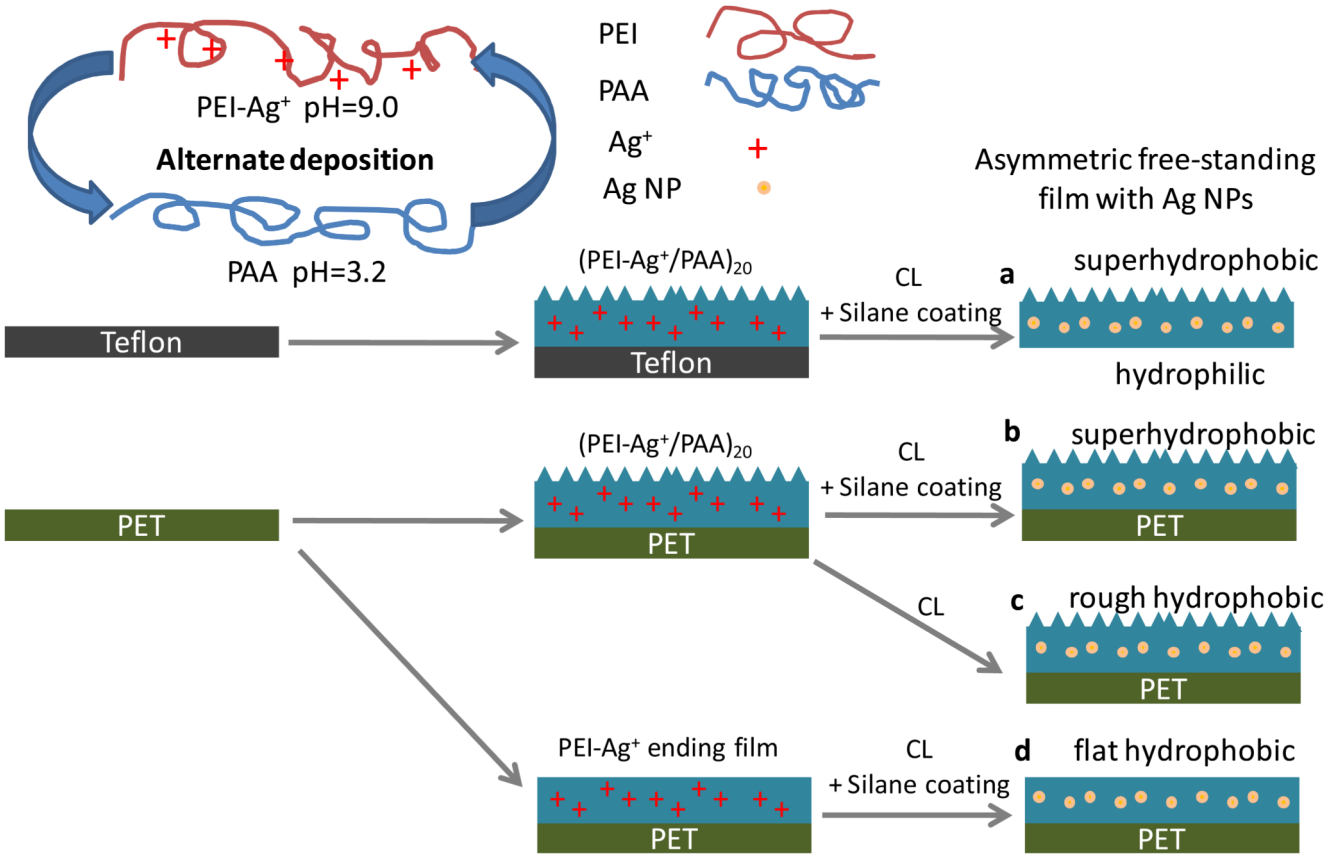

Scheme 1.

Schematic illustration of the fabrication of free-standing (a) and supported (b, c, d) films. Teflon substrate was used to construct free-standing film and PET substrate was used for the supported films. First, the substrates were alternately immersed in PEI-Ag^+ (pH=9.0) and PAA (pH=3.2) solutions to form 20 (a, b, c) or 19.5 (d) bilayered films (PAA-ending films or PEI-Ag^+-ending films). Then, the films were heated in a sealed chamber to be thermally cross-linked (CL) in the presence (a, b, d) or absence (c) of an additional silane coating. Finally, free-standing film with top surface superhydrophobic and bottom surface hydrophilic (a) was obtained from Teflon substrate, and supported superhydrophobic film (b), supported rough hydrophobic film (c) and flat supported hydrophobic film (d) were obtained on PET substrate.

Europe PMC Funders Author Manuscripts

Table 1

Water contact angles for supported and free-standing films. Supported films are made of 40 layers for PAA-ending films, or of 39 layers for PEI-ending films.

	(PEI-Ag/PAA) films on PET		$(PEI-Ag/PAA)_{20}$ free-standing film
	Thermal crosslinking	**Thermal crosslinking + silane coating**	**Thermal crosslinking + silane coating**
PAA-ending	126.2±1.3°	169.2±3.5°	168.2±2.5°[a], 52.7±5.7°[b]
PEI-ending	98.6±0.8°	112.1±1.9°	

[a] measured on the top surface of $(PEI-Ag/PAA)_{20}$ free-standing film

[b] measured on the bottom surface of $(PEI-Ag/PAA)_{20}$ free-standing film